UPPER LIMB BIOMECHANICS USING OPENSIM DURING WHEELCHAIR PROPULSION

Kristy A. Godoy Jaimes, Programa de Engenharia Biomédica COPPE/UFRJ, kristygodoy@peb.ufrj.br
Marcos Duarte, Engenharia Biomédica Universidade Federal do ABC, marcos.duarte@ufabc.edu.br
Luciano Luporini Menegaldo, Programa de Engenharia Biomédica COPPE/UFRJ, lmeneg@peb.ufrj.br

Abstract.

Objective: to estimate upper limb net joint moments during wheelchair propulsion movement using OpenSim´s MoBL-ARMS dynamic upper limb model.

Methods: trials of a person propelling a wheelchair at a comfortable speed were recorded using an infrared video camera system and two SmartWheels adapted to the wheelchair, experimental data was then analyzed using an OpenSim upper limb musculoskeletal model.

Results: mean values for angular kinematics and net joint moments.

Conclusion: upper limb angular kinematics and joint moments were calculated, average max moment found for elbow flexion was -4.74 Nm, shoulder rotation 55.43 Nm, shoulder elevation -19.77 Nm, forearm rotation -1.22 Nm, wrist deviation 6.07 Nm and for wrist flexion 2.22 Nm. Direct comparisons of our results with values reported by other authors was difficult mainly because differences among models and experiment setups of the studies. More trials for the same and different speeds are needed to verify the coherence of the approach.

***Key words**: Wheelchair. Propulsion. Biomechanics. OpenSim. MoBL-ARMS.*

1 INTRODUCTION

Wheelchairs are one of the principal mobility devices around the world, however, a great portion of independent wheelchair users develop upper limb joints injuries caused primarily by the repetitive nature of the movement done to push the wheelchair (van der Woude *et al*. (2001), Boninger *et al.* (1998), Collinger *et al.* (2008), Shimada *et al.* (1998)).

Recording kinematic and dynamic data of a movement and applying it to musculoskeletal models can help to understand the underlying features of pathology mechanisms (Delp *et al.* (2007)), and it has been used to study wheelchair propulsion biomechanics (van der Woude *et al*. (2001)).

Wheelchair manual propulsion movement is cyclical and can be divided in two phases, propulsion and recovery. The propulsion phase is principally denoted by the contact of the hand with the handrim in order to move the wheelchair. The recovery phase starts when the hand releases the rim and finishes just before the hand meets the rim again to start a new cycle (Kwarciak *et al.* (2009), Shimada *et al.* (1998)).

OpenSim is an open-source software system (Delp *et al.* (2007)), that can be fed with experimental data. Some previous works have used the software to investigate musculoskeletal system dynamics both for lower and upper limbs (Hamner *et al.* (2010), Holloway *et al.* (2015)). We used the MoBL-ARMS (Saul *et al.* (2015)) dynamic upper limb model from the software and applied the inverse kinematics and inverse dynamics tools to calculate upper limb angular kinematics and net joints moments.

2 METHODS

A 28 years old subject, 1.67 m tall and 53.38 kg of weight, propelled a wheelchair (M3, Ortobras) at comfortable speed in a straight line, at level floor for a distance that ensured to record at least four propulsion strokes, the number of strokes were verified by visualization after each trial. The reference for comfortable speed was the speed the person uses to cross a street.

The position of reflective markers positioned on anatomic landmarks (Fig. 1) were recorded using a Motion Analysis system with 12 cameras at a frequency of 150 Hz (Raptor-4 Digital RealTime System, Motion Analysis Inc., EUA).

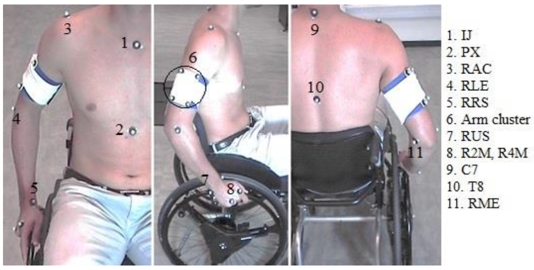

Figure 1. Reflective markers and anatomic landmarks.

Three dimensional forces and moments at the hand-rim interface were obtained using a SmartWheel (Out-Front, Mesa, AZ, USA) adapted to the wheelchair, at a frequency of 240 Hz approximately, one SmartWheel was placed in each side to maintain the same conditions and avoid movement asymmetry.

All the data collection took place at BMClab, the Biomechanics and Motor Control Laboratory of the Biomedical Engineering program at Federal University of ABC (Sao Paulo, Brazil) in 2016, the project was approved by the Research Ethics Committee of the university under the number 1.598.969.

Six trials were analyzed using OpenSim software (version 3.3, http://opensim.stanford.edu/). We used MoBL-ARMS dynamic upper limb model (Saul *et al.* (2015), specifically MoBL_ARMS_module5_scaleIK.osim was modified in order to have the following markers: jugular notch (IJ), xiphoid process (PX), 7th cervical vertebra (C7), right acromion process (RAC), lateral and medial elbow's epicondyles (RLE, RME), radial and ulnar writs' styloid processes (RRS, RUS) and the proximal part of the second metacarpal bone (R2M), see Fig. 2.

The model incorporates seven movements: shoulder rotation and elevation, elbow flexion, forearm rotation, wrist flexion and deviation, and one called elevation plane. The last one is considered when shoulder elevation is not zero.

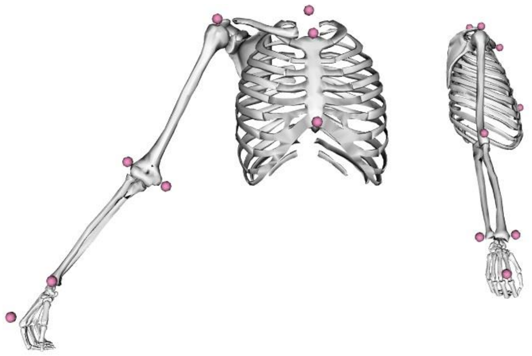

Figure 2. Markers on the modified OpenSim model.

To scale the model length measurements for the sternum, clavicle, humerus, ulna and radius were calculated from pair markers. Arm's mass (3.832 kg) was calculated following the Dempster's body segment parameters Robertson *et al.* (2014).

The inverse kinematics and inverse dynamics tools were applied to the scaled model. Input files (.trc and .mot) were created from the experimental data. Previous to the generation of the input files, raw kinematic and dynamic data were synchronized and filtered by a Butterworth 2nd order filter, cut frequency (between 10 and 13 Hz) was calculated for each trial using residual analysis (Marcos Duarte, https://github.com/demotu/BMC', accessed January 2017), they were also filtered by the built in filter of OpenSim by default value of 6 Hz when the inverse dynamics tool was applied.

3 RESULTS

Mean velocity, propulsion phase average time and average time for a cycle were 1.08 (±0.04) $m.s^{-1}$, 0.44 (±0.10) s, and 1.10 (±0.08) s respectively.

Angular kinematics and net joint moments were obtained for six of the seven degrees of freedom of the model, elevation plane was not included. One cycle of each trial was chosen. Figure (3) show the graphs for the angular kinematics, vertical lines represent the instant when the hand releases the rim and the recovery phase starts. Mean maximum and minimum values and standard deviation are shown in each graph. The trials were not time normalized what could be one of the reasons for the wide time difference in the phase shift.

Table 1 shows some reported moments on the literature, in the last row some maximum average moments found in this work are also reported. The highest value for shoulder elevation moment was -19.77 Nm that showed just before the instant the hand made contact with the rim to start a new cycle, at the same time as the shoulder is close if not at its maximum extension. Average maximum moment for shoulder rotation was 55.43 Nm, internal rotation, it was present close to the time when the hand releases the rim to start the recovery phase. For the elbow, the peak moment was -4.74 Nm, extension, found before the phase shift, same time when the maximum value for wrist ulnar deviation moment occurred, 6.07 Nm.

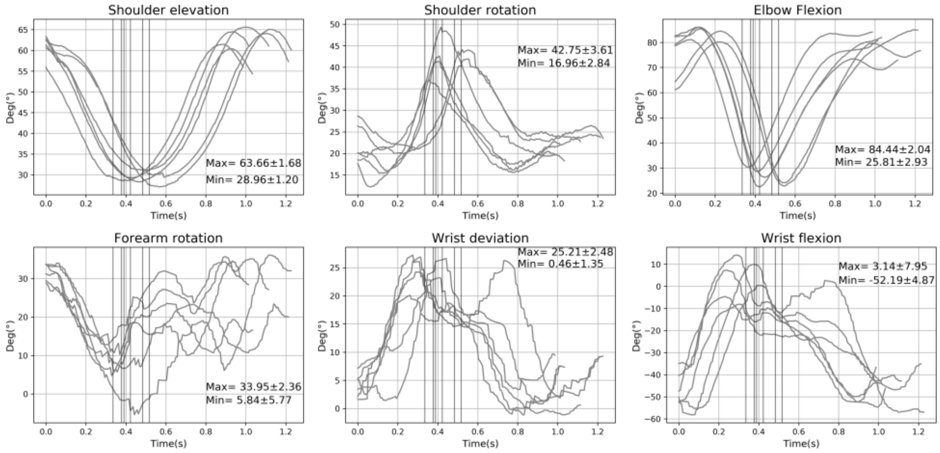

Figure 3. Angular kinematics

Table 1. Some joint moments reported on the literature and reported in this work (last row).

					Shoulder						Elbow						Wrist					
Authors	**N**	**Speed (m/s)**	**Other information**	**Units**	**Add.**	**Abd.**	**Int. rot.**	**Ext. rot.**	**Flex.**	**Ext.**	**Add.**	**Abd.**	**Pron.**	**Sup.**	**Flex.**	**Ext.**	**Ulnar dev.**	**Radial dev.**	**Pron.**	**Sup.**	**Flex.**	**Ext.**
Desroches *et al.* (2010)	9	1.27	mean weight (kg) 61.1; mean arms' length (m) 0.63; force and torque sensing device (TSR)	(Nm/0.5(m_0gl_0))	-	-0.024	0.068	-	0.076	-	0.019	-	0.003	-	0.028	-	0.017	-	-	0.006	-	-0.019
Agudo *et al.* (2010)	51	0.83	Force and torque sensing (SmartWheel) Does not consider scapula, clavicle and thoracic spine movements	Nm	3.275	-4.725	2.625	-1.225	8.200	-5.125	0.875	-1.375	1.150	-2.775	5.025	-0.900	0.125	-0.475	0.250	-0.050	0.300	-0.275
Collinger *et al.* (2008)	61	1.09	Force and torque sensing (SmartWheel)	Nm	7.100	3.200	15.300	5.100	5.400	10.800	-	-	-	-	-	-	-	-	-	-	-	-
Boninger *et al.* (1997)	6	1.3	Subjects were athletes Force and torque sensing (SmartWheel)	Nm	-	-	-	-	-	-	-	-	-	-	-	-	16.600	0.800	1.000	10.000	3.400	5.200
Seonhong *et al.* (2013)	9	Slow	Two groups were analyzed, experienced and novice, here data from experienced was taken into account. Sagittal plane	Nm	-	-	-	-	5.220	-	-	-	-	-	-	-3.010	-	-	-	-	-	-2.310
This paper	1	1.08	Force and torque sensing (SmartWheel) MoBL-ARMS dynamic upper limb model (OpenSim)	Nm	-	-	55.430	-	-	-	-	-	-	-1.22	3.450	-4.740	6.070	-2.040	-	-	2.220	-0.530

Add.=adduction; Abd.=abduction; Int. rot.=internal rotation; Ext. rot.=external rotation; Pron.=pronation; Sup.=supination; Flex.=flexion; Ext.=extension; dev.=deviation

4 DISCUSSION

The range of motion for the degrees of freedom were 34.70º for shoulder elevation, 25.79º for shoulder rotation, 58.63º for elbow flexion, 28.11º for forearm rotation, 24.75º for wrist deviation and 55.33º for wrist flexion, as seen in Fig. 3. It is important to notice the high values of the standard deviation for the wrist flexion, similar characteristic was reported by Boninger *et al.* (1997) where the results showed 7.1º (±5.2) and 7.4º (±7.8) as mean maximum values for 1.3 $m.s^{-1}$ and 2.2 $m.s^{-1}$ respectively, and -38.6º (±8.8) and 34.2º (±7.0) as mean minimum values. They also reported 20.0º (±5.0) and 22.0º (±6.4) mean maximum values for ulnar deviation and 25.1º (±9.0) and 21.4º (±6.9) mean maximum values for radial deviation, this range of motion is almost twice the one reported for our subject. Boninger *et al.* (1998) reported a range of motion of 54.0º and 58.1º for elbow flexion/extension, 37.3º and 44.4º for internal/external rotation of the arm at 0.89 $m.s^{-1}$ and 2.23 $m.s^{-1}$ respectively.

Comparisons among the moments found and the reported in the literature are difficult to address mainly because of the differences among models and experiment setups of the studies (Boninger *et al.* (1998), Agudo *et al.* (2010)). After the inverse dynamics tool was applied, seven different moments were computed and six chosen to be analyzed. In this OpenSim particular model (MoBL-ARMS), the shoulder elevation includes rigid body coupled movements of the scapula and the clavicle, as kinematic functions (Holzbaur *et al.* (2005)). Depending on the position of the elevation plane, the shoulder will elevate anteriorly or posteriorly to the thorax. Therefore, shoulder elevation degree of freedom cannot be specified, as usually, as shoulder extension/flexion or shoulder abduction/adduction, which are the coordinates reported in the literature.

5 CONCLUSION AND FUTURE WORK

Upper limb joint net moments were computed using the MoBL-ARMS OpenSim model. Kinematic results were satisfactory and congruent with results from the literature, on the other hand, net joint moments results, although reasonable, were not easy to compare directly with other results already reported. One limitation of this work is that only one subject was analyzed. More trials with more subjects at different speeds are needed to analyze the consistency of the model in the study of wheelchair propulsion. However, literature about wheelchair propulsion using this OpenSim had not been previously reported at this time, in our knowledge.

6 REFERENCES

AGUDO, G.; ESPINOSA, A.; PÉREZ, E.; PÉREZ, N.S.; RODRÍGUEZ, P.L. Upper limb joint kinetics during manual wheelchair propulsion in patients with different levels of spinal cord injury. **Journal of Biomechanics**, v. 43, p. 2508-15, 2010.

BONINGER, M.L.; COOPER, R.A.; ROBERTSON, R.N.; RUDY, T.E. Wrist biomechanics during two speeds of wheelchair propulsion: an analysis using a local coordinate system. **Archives of Physical Medicine and Rehabilitation**, v. 78, p. 364-72, 1997.

BONINGER, M.L.; COOPER, R.A.; SHIMADA, S.D.; RUDY, T.E. Shoulder and elbow motion during two speeds of wheelchair propulsion: a description using a local coordinate system. **Spinal Cord,** v. 38, p. 418-26, 1998.

COLLINGER, J.L.; BONINGER, M.L.; KOONTZ, A.M.; PRICE, R.; SISTO, S.A.; TOLERICO, M.L.; COOPER, R.A. Shoulder biomechanics during the push phase of wheelchair propulsion: a multisite study of persons with paraplegia. **Archives of Physical Medicine and Rehabilitation**, v. 89, p. 667-76, 2008.

DELP, S.L. *et al*., "OpenSim: Open-Source Software to Create and Analyze Dynamic Simulations of Movement. **IEEE Transactions on Biomedical Engineering**, v. 54, p. 1940-50, 2007.

DESROCHES, G.; DUMAS, R.; PRADON, D.; VASLIN, P.; LEPOUTRE, F.X.; CHÈZE, L. Upper limb joint dynamics during manual wheelchair propulsion. **Clinical Biomechanics**, v. 25, p. 299-306, 2010.

DUARTE, M. Notes on Scientific Computing for Biomechanics and Motor Control. GitHub repository, https://github.com/demotu/BMC, accessed: January 2017.

HAMNER, S.R.; SETH, A.; DELP, S.L.; Muscle contributions to propulsion and support during running. **Journal of Biomechanics**, v.43, p. 2709-16, 2010.

HOLLOWAY, C.S.; SYMONDS, A.; SUZUKI, T.; GALL, A.; SMITHAM, P.; TAYLOR, S. Linking wheelchair kinetics to glenohumeral joint demand during everyday accessibility activities. **Conf Proc IEEE Eng Med Biol Soc**, p. 2478-81, 2015.

HOLZBAUR, K.R.; MURRAY, W.M.; DELP, S.L. A model of the upper extremity for simulating musculoskeletal surgery and analyzing neuromuscular control. **Annals of Biomedical Engineering**, v. 33, p. 829–40, 2005.

KWARCIAK, A. M.; SISTO, S. A.; YAROSSI, M.; PRICE, R.; KOMAROFF, E.; BONINGER, M. L. Redefining the Manual Wheelchair Stroke Cycle: identification and impact of nonpropulsive pushrim contact. **Archives of Physical Medicine and Rehabilitation**, v. 90, p. 20-6, 2009.

SAUL, K.R.; GOEHLER, C.M.; DALY, M.; VIDT, M.E. VELISAR, A.; MURRAY, W.M. Benchmarking of dynamic simulation predictions in two software platforms using an upper limb musculoskeletal model**. Computer Methods in Biomechanics and Biomedical Engineering**, v. 18, p. 1445-58, 2015.

SHIMADA, S.D.; ROBERTSON, R.N.; BONINGER, M.L.; COOPER, R.A. Kinematic characterization of wheelchair propulsion. **Journal of Rehabilitation Research and Development; Washington**, v. 35, p. 210-18, 1998.

VAN DER WOUDE, L.H.V.; VEEGER, H.E.J.; DALLMEIJER, A.J.; JANSSEN, T.W.J.; ROZENDAAL, L.A. Biomechanics and physiology in active manual wheelchair propulsion. **Medical Engineering & Physics**, v. 23, p. 713-33, 2001.

7 ACKNOWLEDGEMENTS

This work was supported by CAPES.